HHS Public Access

Author manuscript

Benef Microbes. Author manuscript; available in PMC 2020 March 12.

Published in final edited form as:

Benef Microbes. 2019 December 09; 10(8): 823–839. doi:10.3920/BM2019.0017.

Bifidobacterium longum-fermented rice bran and rice bran supplementation affects the gut microbiome and metabolome

N.J. Nealon[1,2,#], **K.D. Parker**[1,#], **P. Lahaie**[1], **H. Ibrahim**[1,3], **A.K. Maurya**[4], **K. Raina**[4,5], **E.P. Ryan**[1,2,6]

[1]Department of Environmental and Radiological Health Sciences, College of Veterinary Medicine and Biomedical Sciences, Colorado State University, Fort Collins, CO 80521, USA;

[2]Program in Cellular and Molecular Biology, Colorado State University, Fort Collins, 80521 CO, USA

[3]Zagazig University, Department of Medical Biochemistry, Faculty of Medicine, 44511 Zagazig, Egypt

[4]Skaggs School of Pharmacy and Pharmaceutical Sciences, University of Colorado Denver, Anschutz Medical Campus, Aurora, CO 80045, USA

[5]Department of Pharmaceutical Sciences, South Dakota State University, Brookings, SD 57007, USA

[6]University of Colorado Cancer Center, Division of Cancer Control and Prevention, Aurora, CO 80045, USA

Abstract

This study investigated gut microbiota composition along with food, host, and microbial derived metabolites in the colon and systemic circulation of healthy mice following dietary rice bran and fermented rice bran intake. Adult male BALB/c mice were fed a control diet or one of two experimental diets containing 10% w/w rice bran fermented by *Bifidobacterium longum* or 10% w/w non-fermented rice bran for 15 weeks. Metabolomics was performed on the study diets (food), the murine colon and whole blood. These were analysed in concert with 16S rRNA amplicon sequencing of faeces, caecum, and colon microbiomes. Principal components analysis of murine microbiota composition displayed marked separation between control and experimental diets, and between faecal and tissue (caecum and colon) microbiomes. Colon and caecal microbiomes in both experimental diet groups showed enrichment of *Roseburia, Lachnospiraceae*, and *Clostridiales* related amplicon sequence variants compared to control. Bacterial composition was largely similar between experimental diets. Metabolite profiling revealed 530 small molecules comprising of 39% amino acids and 21% lipids that had differential abundances across food,

e.p.ryan@colostate.edu.

[#]these authors contributed equally to this manuscript

Supplementary material

Supplementary material can be found online at https://doi.org/10.3920/BM2019.0017.

Materials and methods S1.

Additional data and R codes are available in a separate tar. gz file: Code S1, Code S2, Sheet S1, MetaData File S1, and Data File S1-S4.

colon, and blood matrices, and statistically significant between the control, rice bran, and fermented rice bran groups. The amino acid metabolite, N-delta-acetylornithine, was notably increased by *B. longum* rice bran fermentation when compared to non-fermented rice bran in food, colon, and blood. These findings support that dietary intake of rice bran fermented with *B. longum* modulates multiple metabolic pathways important to the gut and overall health.

Keywords

fermentation; microbiome; metabolites; colon; rice bran

1. Introduction

Rice bran, the outer coating of brown rice, contributes the prebiotic, phytochemical and nutritional health benefits of whole grain brown rice. Numerous studies performed in humans and animals have shown colonic health and disease protective functions of a diet rich in rice bran (Henderson *et al.*, 2012a,b; Lei *et al.*, 2016; Sheflin *et al.*, 2015, 2017; Yang *et al.*, 2015). Metabolite profiling of heat-stabilised rice bran has revealed a large suite of bioactive compounds including various amino acids, small peptides, lipids, nucleotides, vitamins and cofactors, and plant phytochemicals available in digestible and non-digestible forms to the host (Zarei *et al.*, 2017). Many rice bran components have previously-reported roles in slowing tumour and pathogen growth via altering cell proliferation, combating oxidative stress, reducing inflammation and modulating the gut microbiome and metabolism (Fabian and Ju, 2011; Law *et al.*, 2017; So *et al.*, 2016; Sohail *et al.*, 2017). Gut commensal microbes have shown the capacity for fermenting rice bran carbohydrates, phytochemicals, lipids and amino acids in animals and people (Sheflin *et al.*, 2017; Tuncil *et al.*, 2018). Emerging evidence supports that rice bran components modulate host and gut microbial metabolism to benefit enterocytes and the mucosal immune system (Brown *et al.*, 2017; Si *et al.*, 2018; Yang *et al.*, 2015; Zarei *et al.*, 2017). Genome sequencing of the faecal microbial communities and identification of small molecule profiles using metabolomics are promising tools to evaluate the effects of dietary interventions broadly (Bazanella *et al.*, 2017; Derkach *et al.*, 2017; Hernandez-Alonso *et al.*, 2017; Lee *et al.*, 2017; McIntosh *et al.*, 2017; Tovar *et al.*, 2017; Vandeputte *et al.*, 2017), and were previously utilised for rice bran (Brown *et al.*, 2017; Henderson *et al.*, 2012a; Sheflin *et al.*, 2015, 2017; Si *et al.*, 2018). However, these studies have not yet advanced our understanding of how rice bran fermentation impacts the colon tissue microbiome and the bioavailability of the fermented food microbial-metabolic components into the colon and systemic circulation.

Globally, lactic acid bacteria are the widest order of microbes involved in food fermentation (Pessione and Cirrincione, 2016), and a variety of these organisms exist as part of the native gut microbiome to confer benefits to the host. *Bifidobacterium* represents another important genus of native gut probiotics that were shown to increase in relative percentages after 28 days of rice bran consumption (30 g/day) by healthy adults alongside modulations to rice bran-derived carbohydrates, phytochemicals, amino acids and lipids (Sheflin *et al.*, 2015), supporting the bifidogenic properties of rice bran components. In a related study with daily rice bran intake by adult colorectal cancer survivors, favourable modulations were captured

in the stool metabolome, including shifts in fatty acid, branched chain amino acid, and B-vitamin metabolism (Brown *et al.*, 2017; Sheflin *et al.*, 2017). Multiple strains of *Bifidobacterium* have been tested in food fermentation and exhibited health effects related to increased production of short chain and branched chain fatty acids that are critical for normal colonocyte function (Bunesova *et al.*, 2016; Celiberto *et al.*, 2017; Gagnon *et al.*, 2015; Kim *et al.*, 2018; Phoem *et al.*, 2015), yet other metabolites contributing to *Bifidobacterium* health promotion need further characterisation.

This study aimed to distinguish host and microbe metabolic impacts of consuming dietary rice bran fermented with *Bifidobacterium longum* from the effects of consuming rice bran or a nutrient-matched control diet. Daily intake of *B. longum*-fermented rice bran for 15-weeks in healthy mice was hypothesised to elicit changes to host and intestinal microbiome metabolism and result in differences between bioactive metabolites in colon tissue and blood. This study used next-generation sequencing approaches to characterise murine caecum, colon, and faecal microbiomes and non-targeted metabolomics to determine metabolite profiles of study diets (food), colon tissue, and whole blood metabolomes of mice consuming each study diet. Multivariate statistical approaches were utilised to assess differential abundance of bacterial amplicon sequence variants and differential production of bioactive compounds with previously reported cancer-protective and antimicrobial functions. Few studies have evaluated the effects of fermented foods on healthy gut microbiomes (Cowan *et al.*, 2014; Zheng *et al.*, 2015), yet none of these studies provided direct comparisons to the non-fermented form of the same food type. Exploiting both microbial sequencing and metabolomics to compare *B. longum* fermented rice bran to rice bran provided a novel, thorough and sensitive analysis for revealing differences in host and gut microbiome metabolism of fermented rice bran versus rice bran. Importantly, fermentation influenced bioavailability of rice bran and microbial digested compounds as these were identified with relevant impacts for intestinal health and enteric disease protection.

2. Materials and methods

Rice bran and food fermentation

Ri300 heat-stabilised rice bran was purchased from Rice Bran Technologies (Sacramento, CA, USA). Rice bran stabilisation took place at 110 °C for 30 min in a commercial dryer as described previously (Forster *et al.*, 2013). Ten kg of rice bran was thoroughly mixed with 10 l of 1.5×10^8 cells/ml of *B. longum* (ATCC-55813; American Type Culture Collection, Manassas, VA, USA) suspended in milliQ water (Millipore Corporation, Burlington, MA, USA). To approximate anaerobic fermentation conditions, the mixture was placed in an airtight stainless-steel pot that was incubated at 37 °C. After 48 h, the resultant slurry was harvested at room temperature and frozen at −20 °C until lyophilisation.

Mouse diet preparation and composition

B. longum-fermented rice bran was thawed and lyophilised overnight using a Labconco Freezone 4.5 Litre Freeze Dry System attached to an Edwards RV5 vacuum pump (Marshall Scientific, Hampton, NH, USA). Mouse diets were prepared as previously described using AIN-93 purified components (Envigo, Madison, WI, USA) as the control diet (Kumar *et al.*,

2012). The heat-stabilised rice bran and the *B. longum*-fermented rice bran was incorporated at 10% w/w into the diets at Envigo. Diets were matched for macronutrient and micronutrient contents with compositions listed in Table 1 and were designed for feeding to healthy adult mice. Briefly, the control diet was composed of 4% w/v corn oil, casein, L-cystine, corn starch, maltodextrin, sucrose, cellulose, mineral and vitamin mix, choline bitartrate, and tertiary butyl-hydroquinone antioxidant. The 10% w/w heat-stabilised rice bran diet and 10% w/w *B. longum*-fermented rice bran diet were adjusted across ingredients to account for nutrients supplied by the rice bran.

Prior to animal feeding, diets were gamma-irradiated (sterilised) to remove pathogens, any viable *B. longum*, and microbial toxins following United States Food and Drug Administration (FDA) protocols (FDA, 2018). Food sterilisation was confirmed using standardised tests for anaerobic plate counts on standard plate count agar (Thermo-Fischer Scientific, Lafayette, CO, USA), for coliform counts on violet red bile agar (Thermo-Fischer Scientific), for *Escherichia coli* counts on violet red bile agar, for mould counts and yeast counts on potato dextrose agar (Thermo-Fischer Scientific), for mesophilic aerobic spore counts and mesophilic anaerobic spore counts on standard plate count agar, and *Salmonella* counts in a 1:9 sample by volume aliquot of lactose broth (Becton-Dickinson, Franklin Lakes, NJ, USA). All microbial enumeration methods followed FDA protocols for microbial testing of foods (Merker, 2018).

Ethics statement

Animal experiments were done under institutional guidelines using approved Institutional Animal Care and Use Committee (IACUC) protocol and an Inter-Institutional Agreement with Colorado State University.

Animal study design and sample collection

Animals were maintained in a specific-pathogen free (SPF) animal housing facility in UC Denver-Anschutz Medical Campus and monitored under an active Sentinel Monitoring Program. Mice were kept under standard conditions in SPF-ventilated isolators with built in systems for free access to water. Pellet diet was added in cage feeders and mice had free access to it. Six-week old male BALB/c mice (Charles River Laboratories, Wilmington, MA, USA) were fed a control AIN-93 pellet diet for a one-week acclimatisation period and then switched to rice bran (n=4), *B. longum*-fermented rice bran (n=4) or maintained on a control diet (n=5) for 15 weeks. During the 15-week feeding phase, faecal samples for each diet group were collected as a function of time for the following time points: 48 h after diet intervention (considered week one), and thereafter on two, six, ten and fourteen weeks after diet intervention. Throughout the study, weekly body weight, diet consumption, and general health of mice was recorded. To avoid cross contamination of microbiota between different groups, only cages of one sub-group were opened under aseptic conditions in an animal transfer station at a given time. At the end of 15-week feeding phase (time of sacrifice), animals were subjected to CO_2 asphyxiation and then euthanised by exsanguination. Whole blood was collected in BD vacutainer K2 EDTA coated tubes (Becton, Dickinson and Company, Franklin Lakes, NJ, USA) and stored at −80 °C. Caecum and its contents were collected, snap frozen, and stored at −80 °C until later use. The entire colon was excised

from the caecum onwards to the distal end and cut open longitudinally along its main axis. Swab samples were collected from the proximal and lower portion of the distal colon and used for microbiome analysis. Next, colons were gently flushed with ice cold saline solution and cleaned with a fine brush to remove remnants of colonic contents. Approximately 2.0–3.0 mm slivers of clean colon tissue from proximal and distal ends were cut, snap frozen, and stored at −80 °C until later use for metabolomics analysis. An overview of the study design and experimental timeline is depicted in Figure 1.

Sample processing, DNA extraction, and 16S rRNA gene sequencing protocols

Lyophilised faecal samples and thawed tissue were homogenised, and 50 mg/sample was used for DNA extraction with the MoBio PowerSoil Kit (MoBio Laboratories Inc., Solana Beach, CA, USA) following manufacturer protocols. Extracted DNA samples were stored at −20 °C until concentration and quality-checking on a NanoDrop 2000 (Thermo-Fisher Scientific). Amplification of the V4 hypervariable region of the 16S rRNA gene and amplicon sequencing on the Illumina MiSeq platform (Illumina Inc., San Diego, CA, USA) followed the standards outlined by the Earth Microbiome Project (Caporaso *et al.*, 2011, 2012), and utilised the 515F/806R (Parada/Aprill) primer pair (Parada *et al.*, 2016; Walters *et al.*, 2016). For full details regarding PCR conditions, product purification, library pooling, and primer sequences see Supplementary materials and methods S1.

Sequence read processing, feature table construction, and taxonomic assignment

Raw single-end FASTQ formatted forward sequence reads were imported into the Quantitative Insights Into Microbial Ecology 2 (QIIME 2; https://qiime2.org/) framework (Caporaso *et al.*, 2010). A feature table comprised of amplicon sequence variant (ASV) absolute abundances for each sample was inferred from reads using the Divisive Amplicon Denoising Algorithm 2 pipeline (Callahan *et al.*, 2016). The feature-classifier plugin was employed for training taxonomic classifiers against 99% operational taxonomic unit (OUT) reference collections from Greengenes 13_8 and SILVA 132, and for assigning taxonomy to each ASV representative sequence (Bokulich *et al.*, 2018; DeSantis *et al.*, 2006; Glockner *et al.*, 2017; McDonald *et al.*, 2012; Quast *et al.*, 2013; Yilmaz *et al.*, 2014). The raw feature table, representative sequence file, and taxonomy tables were exported from QIIME 2 for further processing in R (Bokulich *et al.*, 2018; R-Core-Team, 2018). Following import into R, a master table comprised of hashed feature IDs with corresponding representative sequences, full and truncated Greengenes and SILVA taxonomic lineages, and raw absolute abundances for all features within all samples was constructed using base R in combination with package dplyr (Wickham *et al.*, 2018). This master table served as the entry point for all downstream analysis (Supplementary Datafile S1). To further enhance the quality of the data, features considered potential contaminants (taxonomically assigned as chloroplast, mitochondria, eukaryote; and features without kingdom level assignments) were removed from the master table along with removal of any experimental samples exhibiting excess of 5% relative abundance for the aforementioned contaminant features. Biological samples that sequenced poorly were also removed from the master table. The processed master table was then subset to create three tables containing the appropriate samples needed for analyses presented here (Supplementary DataFile S2, S3 and S4). Samples analysed included 16 negative controls and 41 experimental samples represented by 13 caecum samples, 13 colon

samples (six distal and seven proximal), and 15 faecal samples. Additional methodological details can be found in Supplementary materials and methods S1.

Feature table analyses

To explore whether consumption of *B. longum*-fermented rice bran resulted in enrichment with the *B. longum* fermenting strain, relative abundances for all ASVs assigned to the genus *Bifidobacterium* or lower were visualised using base R and packages dplyr, ggplot2, ggpubr, and reshape2 (Kassambara, 2018; R-Core-Team, 2018; Wickham, 2007; 2016; Wickham *et al.*, 2018). Qualitative comparisons of taxonomy-independent microbiota composition (i.e. composition of all features in a given sample) proceeded using the compositional data analysis paradigm with count zero replacement prior to a ratio transformation to remove the simplex constraint inherent to amplicon sequencing data (Gloor *et al.*, 2017). Zero counts for features were imputed using the count zero multiplicative (CZM) method from R package zCompositions (Palarea-Albaladejo and Martín-Fernández, 2015). CZM adjusted proportions were transformed using the centred log-ratio (clr) transformation followed by ordination with principal components analysis (PCA). PCA plots were constructed using base R along with packages dplyr, ggbiplot, ggplot2, ggpubr, and grid (Kassambara, 2018; R-Core-Team, 2018; Vu, 2011; Wickham, 2016; Wickham *et al.*, 2018). Differential abundance testing of ASVs between study diets was performed using the ALDEx2 R package from the Bioconductor suite (Fernandes *et al.*, 2013, 2014; Gentleman *et al.*, 2004; Huber *et al.*, 2015; Morgan, 2018). Raw *P*-values were produced using the non-parametric Wilcoxon rank-sum test (also called the Mann-Whitney *U* test) comparing each ASV's abundance between two groups (Mann and Whitney, 1947; Wilcoxon, 1945). *P*-values were adjusted for multiple comparisons using the Benjamani-Hochberg procedure to control for false discovery rate (FDR-*P*) (Benjamini and Hochberg, 1995). Any ASV with an expected FDR-*P*-value less than 0.1 was deemed significant. The package BiocParallel from the Bioconductor suite was used to execute ALDEx2 functions using multi-core processing to drastically reduce computational time (Morgan *et al.*, 2019). Colours and colour schemes for all microbiome-centric figures were selected using ColorBrewer 2.0 (Harrower and Brewer, 2003).

Computational details for microbiome analyses

Microbiome analyses were performed on MacOS Mojave 10.14.3, running versions: biom-format 2.1.7, conda 4.5.12, QIIME 2 2018.11.0, Python 3.6.5, R 3.5.3 'Great Truth', R Studio 1.1.463, and R package versions: ALDEx2 1.14.1, BiocParallel 1.16.6, BiocManager 1.30.4, dplyr 0.8.1.1, ggbiplot 0.55, ggplot2 3.1.1, ggpubr 0.2, grid 3.5.3, reshape2 1.4.3, zCompositions 1.2.0.

Public access for microbiome data and analytical materials

Key information from this study was made publicly available to ensure transparency and complete reproducibility of the microbiome analysis performed herein. The amplicon sequence data supporting the conclusions of this manuscript are available via NCBI SRA BioProject Accession PRJNA516457. Sample data are available in Supplementary Metadata File S1. All code for analysis conducted in QIIME 2 are found in Supplementary Code S1. The R code to create the manifest for importing FASTQ files into QIIME 2 is found at the

beginning of Supplementary Code S1. See Supplementary Code S2 for all R code executed downstream of QIIME 2. Any additional methods and detailed methodologies are described in Supplementary materials and methods S1. Each of the materials needed to replicate the entirety of microbiome analysis can also be found on this project's GitHub repository located at github.com/kdprkr/MerlinsManuscript.

Non-targeted metabolomics sample processing

The mouse diets, proximal and distal colon tissues, and whole blood samples were sent to Metabolon Inc© (Durham, NC, USA) for metabolite extraction and metabolite identifications. Mouse diets (200 mg), colon tissue (50 mg) and whole blood (1 ml) were provided on dry ice and were stored at −80 °C until use. Each matrix was extracted with 80% methanol and divided into five equal parts for chromatographic extraction including two rounds of reverse-phase ultra-high performance liquid chromatography tandem mass-spectrometry (UPLC-MS/MS) with positive ion mode electrospray ionisation, one round of reverse-phase UPLC-MS/MS with negative ion mode ESI, one round of hydrophilic-interaction (HILIC)/UPLC-MS/MS with negative ion mode ESI and one backup sample. Aliquots collected under acidic conditions for positive ion mode analysis of hydrophilic compounds were separated on a C18 column (Waters UPLC BEH C18–2.1×100 mm, 1.7 μm; Waters Corporation, Milford, MA, USA) and gradient-eluted using a water and methanol mobile phase with 0.1% v/v formic acid. Aliquots collected under acidic conditions for positive ion mode analysis of hydrophobic compounds were separated on the same column but were gradient eluted with a mobile phase containing water, methanol, 0.05% v/v penta-fluoropropionic anhydride and 0.01% formic acid. Aliquots collected under basic conditions for negative ion ESI were separated using a separate C18 column (Waters UPLC BEH C18–2.1×100 mm, 1.7 μm) and gradient-eluted using a water and acetonitrile mobile phase with 6.5 mM ammonium bicarbonate at pH of eight. The HILIC aliquot was separated using a HILIC column (Waters UPLC BEH Amide 2.1×150 mm, 1.7μm) and gradient-eluted using a water and acetonitrile mobile phase with 10 mM ammonium formate at pH 10.8. Each chromatographically extracted sample was stored overnight under nitrogen gas before mass-spectral analysis, which was performed on a Thermo Scientific Q-Exactive mass spectrometer operated with a heated-ESI source and at a 35,000-mass resolution. Tandem mass spectrometry scans alternated between MS and MSn (high resolution spectral features) scans using dynamic exclusion and covered a range of 70 to 1000 *m/z*. Mass spectral profiles were peak identified and quality-control processed at Metabolon Inc©. Quality control during sample processing was measured by injecting a cocktail of known chemical standards into each sample prior to chromatography and mass spectrometry, via spectral analysis of a pooled matrix sample containing an equal volume of each sample and using extracted water samples as negative controls. Compound identities were made based on an internal library containing over 3,300 commercially available chemical standards and were annotated based on matches to retention time/index, having an *m/z* within 10 ppm to a database standard, and by assessing the overall mass spectral profile matches to database standards. Spectral profiles that were structurally resolved but were otherwise not archived in internal chemical database were reported as 'unknown'.

Metabolomics statistical analysis

Metabolite raw abundances were normalised by dividing the median raw abundance of that metabolite across the entire dataset for each matrix, and to produce median-scaled abundances. For samples lacking a metabolite, the minimum median scaled abundance of that metabolite across the dataset was input as a minimum value before downstream statistical analysis. Metabolite fold differences were calculated for each metabolite by dividing the average median-scaled abundance of the metabolite in one treatment group by that of a second treatment group. All pairs of treatments (rice bran vs control, *B. longum*-rice bran vs control and *B. longum*-rice bran vs rice bran) were analysed for each matrix (i.e. food, colon or blood). UPLC-MS/MS based metabolomics does not allow for cross-matrix statistical analyses because the matrix metabolite abundance profiles have differential median scale values. For the colon tissue, metabolite median-scaled abundances and fold differences were calculated by pooling together proximal and distal colon into a single sample type. For the study diets (food), colon tissue, and blood, median-scaled abundances for each metabolite were compared using two-way analysis of variance (ANOVA) with a Welch's post-hoc test, where significance was defined as $P<0.05$. To account for false discovery rate errors, a *q*-value was calculated for each metabolite and metabolites with a *q*-value less than 0.1 were excluded from downstream analysis.

Metabolic network visualisation

Metabolic network visualisation with Cytoscape Network Analysis version 2.8.3 (https://cytoscape.org/) was performed to compare the abundances of metabolites that were statistically different ($P<0.05$) between *B. longum*-fermented rice bran and rice bran samples in the food, colon tissue, and blood metabolomes. Metabolites were organised into nodal clusters by chemical class (e.g. lipid, amino acid) and were further separated by metabolic pathway (e.g. sphingolipid, polyamine). Node diameters measured the magnitude of each metabolite's fold difference between *B. longum*-fermented rice bran and rice bran samples where larger node diameters reflected larger fold difference magnitudes between *B. longum*-fermented rice bran versus rice bran. Red nodes indicated metabolites that increased in *B. longum*-fermented rice bran versus rice bran and blue nodes indicated metabolites that were significantly decreased. Numbers in nodes are pathway enrichment scores (Pessione and Cirrincione, 2016) that indicate a metabolic pathway's relative contribution of statistically-significant metabolites to treatment differences. Pathway enrichment scores were calculated using the following equation:

$$\mathrm{PES} = \frac{m - k}{N - n}$$

The score is determined by subtracting a pathway's number of statistically-different metabolites (k) from the total number of metabolites in the pathway (m) and then dividing this by the difference in the total number of statistically different metabolites in the entire dataset (n) and the total number of metabolites in the dataset (N). Metabolic pathways with a PES>1.0 containing at least five metabolites, indicated that this pathway had a higher proportion of statistically different metabolites compared to all other pathways and were used to designate pathways contributing to treatment differences.

3. Results

Metabolome differences between control, rice bran and *B. longum* fermented rice bran dietary treatments

Metabolomics of the food identified 663 distinct metabolites that were organised by chemical class and metabolic pathway in Supplementary Table S1 and Sheet S1. A total of 327 metabolites were statistically different in abundances between two or more study diets (Supplementary Table S1). Food metabolites that contributed to the largest treatment differences between the control, rice bran and *B. longum*-fermented rice bran diets are shown in Figure 2, and the metabolite bioactivities are further discussed in Supplementary Table S2. Significant food metabolite changes following fermentation included, but were not limited to lactate, N-delta-acetylornithine, tricarballylate, and salicylate. Lactate is a metabolic end-product of fermentation that was significantly increased ($P<0.05$) in the *B. longum*-fermented rice bran diet compared to the control diet (33.27-fold increase) and to the rice bran diet (95.94-fold increase). The arginine metabolite, N-delta-acetylornithine was 224.67-fold increase in fermented rice bran versus control diet, 170.87-fold-increased in fermented rice bran versus rice bran. Other food compounds contributing to differences between dietary treatments were tricarballylate (2.42-fold increase in rice bran versus control, 3.00-fold increase in fermented rice bran versus control, 1.24-fold increase in fermented rice bran versus rice bran). The rice bran-derived phytochemical, salicylate, had a 5.74-fold increase in rice bran versus control, 7.77fold increase in fermented rice bran versus control, and 1.35-fold increase in fermented rice bran versus rice bran (Figure 2, Supplementary Table S1 and Sheet S1).

Dietary alteration of bacterial composition in the caecum, colon, and faeces of healthy mice

The relative abundance for any ASV sharing taxonomic affiliation with the genus *Bifidobacterium* was used to determine whether an enrichment of the fermenting strain occurred in the microbiomes of mice consuming *B. longum*-fermented rice bran. A total of nine ASVs had *Bifidobacterium* assignments; six were not assigned beyond the genus level, two were identified as *Bifidobacterium pseudolongum*, and one was assigned as *Bifidobacterium bifidum*. The three ASVs with species level assignments were nearly undetectable across microbiomes from all mouse groups, while the six *Bifidobacterium* ASVs were predominantly in faecal samples, independent of study diet (Supplementary Figure S1). These results indicate minimal enrichment of the fermenting strain in the gut microbiomes of mice consuming *B. longum*-fermented rice bran.

Taxonomy-independent murine microbiota composition was qualitatively explored using centred log-ratio transformed ASV abundances ordinated by PCA. These results revealed a separation between faecal microbiomes and microbiomes originating from the caecum and colon, with the latter sample types showing relative similarity to one another (Figure 3A). Comparisons by diet group indicated compositional differences between control and both rice bran and *B. longum*-fermented rice bran groups (Figure 3B). No clear separation was observed between microbiomes of mice fed rice bran or *B. longum*-fermented rice bran

(Figure 3B). Importantly, when negative controls were ordinated alongside diets, these relationships persisted (Supplementary Figure S2).

Given the similarity for proximal and distal colon and caecum microbiomes reported above, these tissues were grouped, and differentially abundant ASVs were assessed in pairwise for all diet combinations using ALDEx2. Thirty differentially abundant ASVs were identified between mice fed a control diet or a rice bran diet; 16 higher in control and 14 higher in rice bran (Supplementary Table S3). 58 differentially abundant ASVs were identified between mice fed a control diet or a *B. longum*-fermented rice bran diet; 36 higher in control and 22 higher in *B. longum*-fermented rice bran (Supplementary Table S3). Six identical ASVs showed higher proportion in both experimental rice bran diets when each was compared to control, while ten identical ASVs were higher in control for both comparisons (Figure 3A and 3B; Supplementary Figure S3A,B). The comparison between rice bran and *B. longum*-fermented rice bran groups revealed two differentially abundant ASVs: a *Roseburia*-related ASV enriched in mice fed *B. longum*-fermented rice bran; and a *Clostridiales*-related ASV enriched in mice fed rice bran (Figure 3C and Supplementary Figure S3C).

Dietary treatments modulate the bioavailability of compounds in the colon metabolome of healthy mice

A total of 664 metabolites were identified in the colon metabolome. The complete list is included in Supplementary Table S1 and Sheet S1, and metabolites that had statistically significant metabolite differences between one or more treatment pairwise analyses are listed in Supplementary Table S1. Amino acid, energy, and lipid metabolites contributed to large treatment differences observed across mice consuming the different foods that were dually associated with health functions (Figure 4, Supplementary Table S2). The arginine metabolite N-delta-acetylornithine, which was elevated in the *B. longum* fermented rice bran diet, was increased 11.18-fold in the colon of fermented rice bran fed mice versus control and elevated 11.77-fold in the colon of mice consuming fermented rice bran versus rice bran. Similarly, tricarballylate, which was elevated in the *B. longum*-fermented rice bran diet compared to the rice bran and control diets, exhibited a 23.34-fold increase in colon of mice consuming the fermented rice bran versus rice bran diets. The lipid 4-cholesten-3-one, which was not differentially abundant across the three food metabolomes, was significantly-decreased (0.74-fold) in the colon tissue of *B. longum*-fermented rice bran versus rice bran-consuming mice and represented a potential host and gut-microbiota-altered metabolite that was influenced by dietary treatment.

Dietary treatments differentially modulate the blood metabolome of healthy mice

A total of 802 metabolites were identified in the blood metabolome (Supplementary Table S1 and Sheet S1) and there were 154 blood metabolites that had significantly different ($P<0.05$) abundances between two or more treatments (Supplementary Table S1). Metabolites that distinguished the blood metabolome for each of the diet group comparisons are shown in Table 2, and the bioactivities for selected metabolites are described in Supplementary Table S2. N-delta-acetyl-ornithine, which was elevated in the *B. longum*-fermented rice bran and rice bran diets, as well as in the colon tissue of mice consuming fermented rice bran and rice bran, was increased 2.16-fold in the blood of mice consuming

the rice bran diet versus the control diet, increased 9.59-fold in mice consuming the fermented rice bran diet versus the rice bran diet, and also was elevated 4.44-fold in the blood of mice consuming the fermented rice bran versus rice bran diets. Ferulic acid 4-sulphate and 4-methoxyphenol sulphate represent rice bran phytochemicals that were modified by gut microbes and showed elevated levels in blood. Ferulic acid 4-sulphate had 80.32-fold increase for *B. longum* rice bran and 73.77-fold increase for rice bran when compared to control diet fed mice. Alterations in host-produced primary bile acids and microbiota-derived secondary bile acids were also observed in the blood metabolome for the primary bile acid, chenodeoxycholate. Chenodeoxycholate showed a 1.79-fold increase in the blood of mice consuming the *B. longum* fermented rice bran versus rice bran diet. The secondary bile acid deoxycholate decreased 0.78-fold in the blood of mice consuming the fermented rice bran versus control diet and 1.49-fold-increased in the blood of mice consuming the *B. longum*-fermented rice bran versus rice bran diets.

4. Discussion

We examined daily dietary intake of *B. longum*-fermented rice bran for metabolic distinctions to non-fermented rice bran or a control diet intake for 15 weeks in healthy mice. Dietary interventions were assessed for effects on gut bacterial community composition and for uptake of metabolic by-products into the host via metabolite measures in colon tissue and blood. When comparing the metabolite profiles of all three diets, considerable differences existed in the food metabolomes of *B. longum*-fermented rice bran versus non-fermented rice bran and this comparison was explored further for metabolites that are not heavily characterised in fermented foods for health functions. The healthy murine dietary exposure for 15-weeks was a key aspect of this investigation as colon microbiome composition, and blood and colon metabolite profiles were not challenged by chemicals or pathogens, and thus the differences identified in the colon tissue and blood metabolomes between mice fed *B. longum*-fermented rice bran versus the non-fermented rice bran have strong implications for metabolic mechanisms by which food fermentation promote gut health and to prevent chronic and infectious enteric diseases.

Compositional analysis of caecum and colon microbiomes indicated clear differences between mice fed a control diet and mice fed with either rice bran or *B. longum*-fermented rice bran; however, the differences between experimental diets were limited. The sequencing methodologies employed in this study did not differentiate between metabolically active, dormant, or dead prokaryotic organisms (Emerson *et al.*, 2017). The low abundance of *Bifibacterium* spp. in caecum and colon microbiomes and the similar abundance in faecal microbiomes across all study diets indicated nominal, enrichment of the fermenting strain in microbiomes of mice consuming *B. longum*-fermented rice bran. One of the two ASV's identified as differentially abundant between experimental diets was taxonomically assigned to the genus *Roseburia* exhibited enrichment in mice fed a *B. longum*-fermented rice bran diet. This was of particular interest because *Roseburia* are known to produce beneficial short-chain fatty acids, in addition to other compounds exerting anti-inflammatory activity in the gut (Tamanai-Shacoori *et al.*, 2017). Reduced abundance or loss of *Roseburia* spp. have been associated with a variety of diseases, including colorectal cancer (Rezasoltani *et al.*, 2018). An additional differentially abundant ASV represented by *Roseburia* was identified

for paired comparisons of each experimental diet to control and showed strong association with rice bran and *B. longum*-fermented rice bran fed mice. The enrichment of *Roseburia* ASVs may, in part, be explained by the partial hydrolysis of rice bran components created by *B. longum* during fermentation and/or by existing gut microbiota following consumption of either the non-fermented or fermented foods.

These subtle microbiome compositional changes by dietary supplementation with fermented and non-fermented rice bran were further supported by differences in food, microbe and host derived metabolites in the diets, colon and blood. Microbial metabolism was the key contributor to metabolite profile differences between the experimental groups. These compounds collectively had reported antioxidant, immune-modulatory, gut barrier protective, anti-toxicant functions, and many of these were reported in the context of colorectal cancer protection and antimicrobial activities. Among these bioactive food-derived metabolites was N-delta-acetylornithine. The increased colon and blood bioavailability of N-delta-acetylornithine in mice consuming fermented rice bran versus rice bran diets was supported by the substantially increased abundance in the food when comparing these two groups (170.87-fold increase in fermented rice bran food versus rice bran food. Previous studies have shown that some colorectal cancer tumours had lower levels of N-delta-acetylornithine when compared to levels in health mucosal colonocytes (Gómez de Cedrón *et al.*, 2017), suggesting that depletion of this metabolite may either promote or facilitate the dysregulated metabolism associated with colorectal cancer pathogenesis. Given its high levels in fermented rice bran versus rice bran in colon and blood, N-delta-acetylornithine merits mechanistic examination as a fermented food-associated compound and for its effects on host colonocytes. Microbial fermentation-mediated release of N-delta-acetylornithine from rice bran can be assessed using other probiotic fermentation starter cultures to optimise its yield in food products. N-delta-acetylornithine can additionally be explored for its utility as a biomarker of fermented rice bran consumption.

Tricarballylate, which was elevated in both the rice bran and *B. longum*-fermented rice bran diets compared to the control diet, as well as in the fermented rice bran diet versus the rice bran diet, was also elevated 23.34-fold in the colon tissue of mice consuming fermented rice bran versus rice bran. In previous studies, dietary-derived tricarballylate functioned as an aconitase inhibitor that decreased the conversion of citrate into isocitrate, and reduced metabolite flux through the tricarboxylic acid cycle to decrease *Salmonella* Typhimurium growth (Nealon *et al.*, 2017; Watson *et al.*, 1969). Exogenous tricarballylate administered to rats resulted in decreased succinate production by colonocytes (Wolffram *et al.*, 1994), suggesting that tricarballylate could modulate energy balance. Given that increased tricarboxylic acid cycle activity has been reported in multiple cancer types and in several lines of chemotherapy-resistant neoplastic colonocytes (Zhou *et al.*, 2012), dietary sources of tricarballylate warrant investigation for protection against colorectal cancer.

Fermented foods, including tricarballylate-rich *B. longum*-fermented rice bran, especially merit examination for cancer-protective effects because a decreased luminal pH has been associated with enhanced tricarballylate uptake into colonocytes (Zhou *et al.*, 2012). Future investigations should consider measurements of colonic pH following consumption of rice

bran and *B. longum* fermented rice bran, as pH may exert bidirectional influences on colon tissue metabolites (e.g. tricarballylate levels) that can be modulated by fermented foods.

While the *B. longum*-fermented rice bran diet metabolites delivered different levels of bioactive metabolites to the host compared to the rice bran diet, differential metabolism also occurred for fermented rice bran versus rice bran by the host and gut microbiota. For example, the bile acid precursor 4-cholesten-3-one was not differentially abundant between the *B. longum*-fermented and rice bran diets, but it was significantly lowered in the colon tissue of mice consuming fermented rice bran. Mammals and many bacteria metabolise 4-cholesten-3-one to synthesise steroid compounds, including bile acids (Wu *et al.*, 2015). One explanation for the decreased colonic 4-cholesten-3-one levels in mice consuming *B. longum*-fermented rice bran could be explained by concurrent elevations of the primary bile acid chenodeoxycholate (1.79-fold increased) and the secondary bile acid deoxycholate (1.49-fold increase) in the blood when compared to mice consuming rice bran alone. These are downstream bile acids produced by mammals and the microbiota respectively. In the context of health-promoting effects, these metabolic shifts in 4-cholesten-3-one metabolism by *B. longum*-fermented rice bran consumption may function to decrease intestinal inflammation. In a previous human study, elevated colon tissue levels of 4-cholesten-3-one were associated with increased pro-inflammatory cytokine responses by the mucosal immune system, and 4-cholesten-3-one was significantly-increased in the faeces of adults with colorectal cancer versus healthy adults (Chen *et al.*, 2017a). Given that chronic inflammation facilitates both tumour initiation and promotion in colorectal cancer (Chen *et al.*, 2017b), the reduced colonic inflammatory cascades facilitated by consumption of *B. longum* fermented rice bran support that this may be a valuable dietary aid that can modulate host and microbiota metabolism to support gut health and prevent disease.

5. Conclusions

Metabolome comparisons of fermented foods alongside the non-fermented forms have been largely unexplored using non-targeted approaches and merited evaluation herein before and after metabolism by the murine gastrointestinal tract. The *B. longum*-fermented rice bran and the non-fermented rice bran did considerably modulate the healthy murine faecal, caecal, or colon microbiomes when compared to control diets. While only modest differences in composition were noted between the non-fermented rice bran and *B. longum*-fermented rice bran, there were a suite of unique food and microbial-derived metabolites in the colon and bloodstream indicating substantial modulation of host and gut microbiome metabolism. Most metabolic changes involved amino acids and lipids, which supported that gut fermentation enhances bioavailability of rice bran components for promoting colon health. This study design and methodology employed has tremendous potential for testing metabolic differences between probiotic strains and for optimisation of rice bran to have prophylactic and therapeutic use in gastrointestinal disorders across the lifespan. Additional investigations for *B. longum*-fermented rice bran are needed with respect to protection against colon carcinogenesis and infection with gut pathogens. The network of host and gut-microbial mediated metabolic changes by rice bran and fermentation with probiotics merits exploration using metatranscriptomics and metaproteomics. The coordinated and integrated assessment of multiple tissues from a healthy murine host that was fed rice bran in a

fermented and nonfermented form was a rigorous, cross-kingdom scientific approach that has promising applications for many other food types that may support health of mammalian systems with intact gut microbiomes.

Supplementary Material

Refer to Web version on PubMed Central for supplementary material.

Acknowledgements

The authors thank Renee C. Oppel for technical assistance and preparation of the *B. longum*-fermented rice bran diet. Funding for this study was provided by the National Institutes of Health-National Cancer Institute (1R01CA201112–02) as a multi-investigator award of E.P. Ryan and K. Raina. Lastly, we wish to thank all of the mice sacrificed in the work presented here for their contributions towards the pursuit of understanding.

References

Bazanella M, Maier TV, Clavel T, Lagkouvardos I, Lucio M, Maldonado-Gomez MX, Autran C, Walter J, Bode L, Schmitt-Kopplin P. and Haller D, 2017 Randomized controlled trial on the impact of early-life intervention with bifidobacteria on the healthy infant fecal microbiota and metabolome. American Journal of Clinical Nutrition 106: 1274–1286. 10.3945/ajcn.117.157529 [PubMed: 28877893]

Benjamini Y. and Hochberg Y, 1995 Controlling the false discovery rate: a practical and powerful approach to multiple testing. Journal of the Royal Statistical Society Series B 57: 289–300.

Bokulich NA, Kaehler BD, Rideout JR, Dillon M, Bolyen E, Knight R, Huttley GA and Gregory Caporaso J, 2018 Optimizing taxonomic classification of marker-gene amplicon sequences with QIIME 2's q2-feature-classifier plugin. Microbiome 6: 90 10.1186/s40168-018-0470-z [PubMed: 29773078]

Brown DG, Borresen EC, Brown RJ and Ryan EP, 2017 Heat-stabilised rice bran consumption by colorectal cancer survivors modulates stool metabolite profiles and metabolic networks: a randomised controlled trial. British Journal of Nutrition 117: 1244–1256. 10.1017/s0007114517001106 [PubMed: 28643618]

Bunesova V, Lacroix C. and Schwab C, 2016 Fucosyllactose and L-fucose utilization of infant Bifidobacterium longum and Bifidobacterium kashiwanohense. BMC Microbiology 16: 248–248. 10.1186/s12866-016-0867-4 [PubMed: 27782805]

Callahan BJ, McMurdie PJ, Rosen MJ, Han AW, Johnson AJ and Holmes SP, 2016 DADA2: High-resolution sample inference from Illumina amplicon data. Nature Methods 13: 581–583. 10.1038/nmeth.3869 [PubMed: 27214047]

Caporaso JG, Kuczynski J, Stombaugh J, Bittinger K, Bushman FD, Costello EK, Fierer N, Peña AG, Goodrich JK, Gordon JI, Huttley GA, Kelley ST, Knights D, Koenig JE, Ley RE, Lozupone CA, McDonald D, Muegge BD, Pirrung M, Reeder J, Sevinsky JR, Turnbaugh PJ, Walters WA, Widmann J, Yatsunenko T, Zaneveld J. and Knight R, 2010 QIIME allows analysis of high-throughput community sequencing data. Nature Methods 7: 335–336. 10.1038/nmeth.f.303 [PubMed: 20383131]

Caporaso JG, Lauber CL, Walters WA, Berg-Lyons D, Huntley J, Fierer N, Owens SM, Betley J, Fraser L, Bauer M, Gormley N, Gilbert JA, Smith G. and Knight R, 2012 Ultra-high-throughput microbial community analysis on the Illumina HiSeq and MiSeq platforms. ISME Journal 6: 1621 10.1038/ismej.2012.8 [PubMed: 22402401]

Caporaso JG, Lauber CL, Walters WA, Berg-Lyons D, Lozupone CA, Turnbaugh PJ, Fierer N. and Knight R, 2011 Global patterns of 16S rRNA diversity at a depth of millions of sequences per sample. Proceedings of the National Academy of Sciences of the USA 108: 4516 10.1073/pnas.1000080107 [PubMed: 20534432]

Celiberto LS, Bedani R, Dejani NN, Ivo de Medeiros A, Sampaio Zuanon JA, Spolidorio LC, Tallarico Adorno MA, Amancio Varesche MB, Carrilho Galvao F, Valentini SR, Font de Valdez G, Rossi

EA and Cavallini DCU, 2017 Effect of a probiotic beverage consumption (Enterococcus faecium CRL 183 and Bifidobacterium longum ATCC 15707) in rats with chemically induced colitis. PLoS ONE 12: e0175935. 10.1371/journal.pone.0175935

Chen CL, Wu DC, Liu MY, Lin MW, Huang HT, Huang YB, Chen LC, Chen YY, Chen JJ, Yang PH, Kao YC and Chen PY, 2017a Cholest-4-en-3-one attenuates TGF-beta responsiveness by inducing TGF-beta receptors degradation in Mv1Lu cells and colorectal adenocarcinoma cells. Journal of Receptor and Signal Transduction Research 37: 189–199. 10.1080/10799893.2016.1203944 [PubMed: 27401208]

Chen J, Pitmon E. and Wang K, 2017b Microbiome, inflammation and colorectal cancer. Seminars in Immunology 32: 43–53. 10.1016/j.smim.2017.09.006 [PubMed: 28982615]

Cowan TE, Palmnas MS, Yang J, Bomhof MR, Ardell KL, Reimer RA, Vogel HJ and Shearer J, 2014 Chronic coffee consumption in the diet-induced obese rat: impact on gut microbiota and serum metabolomics. Journal of Nutritional Biochemistry 25: 489–495. 10.1016/j.jnutbio.2013.12.009 [PubMed: 24629912]

Derkach A, Sampson J, Joseph J, Playdon MC and Stolzenberg-Solomon RZ, 2017 Effects of dietary sodium on metabolites: the Dietary Approaches to Stop Hypertension (DASH)-Sodium Feeding Study. American Journal of Clinical Nutrition 106: 1131–1141. 10.3945/ajcn.116.150136 [PubMed: 28855223]

DeSantis TZ, Hugenholtz P, Larsen N, Rojas M, Brodie EL, Keller K, Huber T, Dalevi D, Hu P. and Andersen GL, 2006 Greengenes, a chimera-checked 16S rRNA gene database and workbench compatible with ARB. Applied and Environmental Microbiology 72: 5069–5072. 10.1128/aem.03006-05 [PubMed: 16820507]

Emerson JB, Adams RI, Roman CMB, Brooks B, Coil DA, Dahlhausen K, Ganz HH, Hartmann EM, Hsu T, Justice NB, Paulino-Lima IG, Luongo JC, Lymperopoulou DS, Gomez-Silvan C, Rothschild-Mancinelli B, Balk M, Huttenhower C, Nocker A, Vaishampayan P. and Rothschild LJ, 2017 Schrodinger's microbes: tools for distinguishing the living from the dead in microbial ecosystems. Microbiome 5: 86 10.1186/s40168-017-0285-3 [PubMed: 28810907]

Fabian C. and Ju YH, 2011 A review on rice bran protein: its properties and extraction methods. Critical Reviews in Food Science and Nutrition 51: 816–827. 10.1080/10408398.2010.482678 [PubMed: 21888532]

Fernandes AD, Macklaim JM, Linn TG, Reid G. and Gloor GB, 2013 ANOVA-like differential expression (ALDEx) analysis for mixed population RNA-Seq. PLoS ONE 8: e67019-e67019. 10.1371/journal.pone.0067019

Fernandes AD, Reid JN, Macklaim JM, McMurrough TA, Edgell DR and Gloor GB, 2014 Unifying the analysis of high-throughput sequencing datasets: characterizing RNA-seq, 16S rRNA gene sequencing and selective growth experiments by compositional data analysis. Microbiome 2: 15 10.1186/2049-2618-2-15 [PubMed: 24910773]

Food and Drug Administration (FDA), 2018 Irradiation in the production, processing, and handling of animal feed and pet food: subpart B – radiation and radiation sources. Code of Federal Regulations Title 21. Food and Drug Administration, Silver Spring, Maryland, USA.

Forster GM, Raina K, Kumar A, Kumar S, Agarwal R, Chen MH, Bauer JE, McClung AM and Ryan EP, 2013 Rice varietal differences in bioactive bran components for inhibition of colorectal cancer cell growth. Food Chemistry 141: 1545–1552. 10.1016/j.foodchem.2013.04.020 [PubMed: 23790950]

Gagnon M, Savard P, Rivière A, LaPointe G. and Roy D, 2015 Bioaccessible antioxidants in milk fermented by Bifidobacterium longum subsp. longum strains. BioMed Research International 2015: 169381–169381. 10.1155/2015/169381

Gentleman RC, Carey VJ, Bates DM, Bolstad B, Dettling M, Dudoit S, Ellis B, Gautier L, Ge Y, Gentry J, Hornik K, Hothorn T, Huber W, Iacus S, Irizarry R, Leisch F, Li C, Maechler M, Rossini AJ, Sawitzki G, Smith C, Smyth G, Tierney L, Yang JY and Zhang J, 2004 Bioconductor: open software development for computational biology and bioinformatics. Genome Biology 5: R80 10.1186/gb-2004-5-10-r80 [PubMed: 15461798]

Glockner FO, Yilmaz P, Quast C, Gerken J, Beccati A, Ciuprina A, Bruns G, Yarza P, Peplies J, Westram R. and Ludwig W, 2017 25 years of serving the community with ribosomal RNA gene

reference databases and tools. Journal of Biotechnology 261: 169–176. 10.1016/j.jbiotec.2017.06.1198 [PubMed: 28648396]

Gloor GB, Macklaim JM, Pawlowsky-Glahn V. and Egozcue JJ, 2017 Microbiome datasets are compositional: and this is not optional. Frontiers in Microbiology 8: 2224 10.3389/fmicb.2017.02224 [PubMed: 29187837]

Gómez de Cedrón M, Acín Pérez R, Sánchez-Martínez R, Molina S, Herranz J, Feliu J, Reglero G, Enríquez JA and Ramírez de Molina A, 2017 MicroRNA-661 modulates redox and metabolic homeostasis in colon cancer. Molecular Oncology 11: 1768–1787. 10.1002/1878-0261.12142 [PubMed: 28981199]

Harrower M. and Brewer C, 2003 ColorBrewer.org: an online tool for selecting colour schemes for maps. Cartographic Journal 40: 27–37. 10.1179/000870403235002042

Henderson AJ, Kumar A, Barnett B, Dow SW and Ryan EP, 2012a Consumption of rice bran increases mucosal immunoglobulin A concentrations and numbers of intestinal Lactobacillus spp. Journal of Medicinal Food 15: 469–475. 10.1089/jmf.2011.0213 [PubMed: 22248178]

Henderson AJ, Ollila CA, Kumar A, Borresen EC, Raina K, Agarwal R. and Ryan EP, 2012b Chemopreventive properties of dietary rice bran: current status and future prospects. Advanced Nutrition 3: 643–653. 10.3945/an.112.002303

Hernandez-Alonso P, Canueto D, Giardina S, Salas-Salvado J, Canellas N, Correig X. and Bullo M, 2017 Effect of pistachio consumption on the modulation of urinary gut microbiota-related metabolites in prediabetic subjects. Journal of Nutritional Biochemistry 45: 48–53. 10.1016/j.jnutbio.2017.04.002 [PubMed: 28432876]

Huber W, Carey VJ, Gentleman R, Anders S, Carlson M, Carvalho BS, Bravo HC, Davis S, Gatto L, Girke T, Gottardo R, Hahne F, Hansen KD, Irizarry RA, Lawrence M, Love MI, MacDonald J, Obenchain V, Oles AK, Pages H, Reyes A, Shannon P, Smyth GK, Tenenbaum D, Waldron L. and Morgan M, 2015 Orchestrating high-throughput genomic analysis with bioconductor. Nature Methods 12: 115–121. 10.1038/nmeth.3252 [PubMed: 25633503]

Kassambara A, 2018 ggpubr: 'ggplot2' based publication ready plots. Available at: https://rpkgs.datanovia.com/ggpubr/

Kim JM, Ku S, Kim YS, Lee HH, Jin H, Kang S, Li R, Johnston VT, Park SM and Ji EG 2018 Safety evaluations of Bifidobacterium bifidum BGN4 and Bifidobacterium longum BORI. International Journal of Molecular Sciences 19: 1422 10.3390/ijms19051422

Kumar A, Henderson A, Forster GM, Goodyear AW, Weir TL, Leach JE, Dow SW and Ryan EP, 2012 Dietary rice bran promotes resistance to Salmonella enterica serovar Typhimurium colonization in mice. BMC Microbiology 12: 71 10.1186/1471-2180-12-71 [PubMed: 22583915]

Law BMH, Waye MMY, So WKW and Chair SY, 2017 Hypotheses on the potential of rice bran intake to prevent gastrointestinal cancer through the modulation of oxidative stress. International Journal of Molecular Sciences 18: 1352 10.3390/ijms18071352

Lee T, Clavel T, Smirnov K, Schmidt A, Lagkouvardos I, Walker A, Lucio M, Michalke B, Schmitt-Kopplin P, Fedorak R. and Haller D, 2017 Oral versus intravenous iron replacement therapy distinctly alters the gut microbiota and metabolome in patients with IBD. Gut 66: 863–871. 10.1136/gutjnl-2015-309940 [PubMed: 26848182]

Lei S, Ramesh A, Twitchell E, Wen K, Bui T, Weiss M, Yang X, Kocher J, Li G, Giri-Rachman E, Trang NV, Jiang X, Ryan EP and Yuan L, 2016 High protective efficacy of probiotics and rice bran against human norovirus infection and diarrhea in gnotobiotic pigs. Frontiers in Microbiology 7: 1699 10.3389/fmicb.2016.01699 [PubMed: 27853451]

Mann HB and Whitney DR, 1947 On a test of whether one of two random variables is stochastically larger than the other. Annals of Mathematical Statistics 18: 50–60. 10.1214/aoms/1177730491

McDonald D, Price MN, Goodrich J, Nawrocki EP, DeSantis TZ, Probst A, Andersen GL, Knight R. and Hugenholtz P, 2012 An improved Greengenes taxonomy with explicit ranks for ecological and evolutionary analyses of bacteria and archaea. ISME Journal 6: 610–618. 10.1038/ismej.2011.139 [PubMed: 22134646]

McIntosh K, Reed DE, Schneider T, Dang F, Keshteli AH, De Palma G, Madsen K, Bercik P. and Vanner S, 2017 FODMAPs alter symptoms and the metabolome of patients with IBS: a

randomised controlled trial. Gut 66: 1241–1251. 10.1136/gutjnl-2015-311339 [PubMed: 26976734]

Merker RI, 2018 Bacteriological analytical manual. Nutrition. Food and Drug Administration, Silver Spring, MD, USA.

Morgan M, 2018 BiocManager: access the Bioconductor project package repository. R package version 3.9.0. 10.18129/B9.bioc.BiocVersion

Morgan M, Obenchain V, Lang M, Thompson R. and Turaga N, 2019 BiocParallel: Bioconductor facilities for parallel evaluation. 10.18129/B9.bioc.BiocParallel

Nealon NJ, Worcester CR and Ryan EP, 2017 Lactobacillus paracasei metabolism of rice bran reveals metabolome associated with Salmonella Typhimurium growth reduction. Journal of Applied Microbiology 122: 1639–1656. 10.1111/jam.13459 [PubMed: 28371001]

Palarea-Albaladejo J. and Martín-Fernández J, 2015 zCompositions – R package for multivariate imputation of left-censored data under a compositional approach. Chemometrics and Intelligent Laboratory Systems 143: 85–96. 10.1016/j.chemolab.2015.02.019

Parada AE, Needham DM and Fuhrman JA, 2016 Every base matters: assessing small subunit rRNA primers for marine microbiomes with mock communities, time series and global field samples. Environmental Microbiology 18: 1403–1414. 10.1111/1462-2920.13023 [PubMed: 26271760]

Pessione E. and Cirrincione S, 2016 Bioactive molecules released in food by lactic acid bacteria: encrypted peptides and biogenic amines. Frontiers in Microbiology 9(7): 876 10.3389/fmicb.2016.00876

Phoem AN, Chanthachum S. and Voravuthikunchai SP, 2015 Applications of microencapsulated Bifidobacterium longum with Eleutherine americana in fresh milk tofu and pineapple juice. Nutrients 7: 2469–2484. 10.3390/nu7042469 [PubMed: 25854832]

Quast C, Pruesse E, Yilmaz P, Gerken J, Schweer T, Yarza P, Peplies J. and Glockner FO, 2013 The SILVA ribosomal RNA gene database project: improved data processing and web-based tools. Nucleic Acids Research 41: D590–596. 10.1093/nar/gks1219 [PubMed: 23193283]

R-Core-Team, 2018 R: a language and environment for statistical computing. R Foundation for Statistical Computing, Vienna, Austria.

Rezasoltani S, Asadzadeh Aghdaei H, Dabiri H, Akhavan Sepahi A, Modarressi MH and Nazemalhosseini Mojarad E, 2018 The association between fecal microbiota and different types of colorectal polyp as precursors of colorectal cancer. Microbial Pathogenesis 124: 244–249. 10.1016/j.micpath.2018.08.035 [PubMed: 30142468]

Sheflin AM, Borresen EC, Kirkwood JS, Boot CM, Whitney AK, Lu S, Brown RJ, Broeckling CD, Ryan EP and Weir TL, 2017 Dietary supplementation with rice bran or navy bean alters gut bacterial metabolism in colorectal cancer survivors. Molecular Nutrition and Food Research 61: 1500905. 10.1002/mnfr.201500905

Sheflin AM, Borresen EC, Wdowik MJ, Rao S, Brown RJ, Heuberger AL, Broeckling CD, Weir TL and Ryan EP, 2015 Pilot dietary intervention with heat-stabilized rice bran modulates stool microbiota and metabolites in healthy adults. Nutrients 7: 1282–1300. 10.3390/nu7021282 [PubMed: 25690418]

Si X, Shang W, Zhou Z, Shui G, Lam SM, Blanchard C. and Strappe P, 2018 Gamma-aminobutyric acid enriched rice bran diet attenuates insulin resistance and balances energy expenditure via modification of gut microbiota and short-chain fatty acids. Journal of Agricultural and Food Chemistry 66: 881–890. 10.1021/acs.jafc.7b04994 [PubMed: 29327584]

So WKW, Law BMH, Law PTW, Chan CWH and Chair SY, 2016 Current hypothesis for the relationship between dietary rice bran intake, the intestinal microbiota and colorectal cancer prevention. Nutrients 8: 569 10.3390/nu8090569

Sohail M, Rakha A, Butt MS, Iqbal MJ and Rashid S, 2017 Rice bran nutraceutics: a comprehensive review. Critical Reviews in Food Science and Nutrition 57: 3771–3780. 10.1080/10408398.2016.1164120 [PubMed: 27015585]

Tamanai-Shacoori Z, Smida I, Bousarghin L, Loreal O, Meuric V, Fong SB, Bonnaure-Mallet M. and Jolivet-Gougeon A, 2017 Roseburia spp.: a marker of health? Future Microbiology 12: 157–170. 10.2217/fmb-2016-0130 [PubMed: 28139139]

Tovar J, De Mello VD, Nilsson A, Johansson M, Paananen J, Lehtonen M, Hanhineva K. and Bjorck I, 2017 Reduction in cardiometabolic risk factors by a multifunctional diet is mediated via several branches of metabolism as evidenced by nontargeted metabolite profiling approach. Molecular Nutrition and Food Research 61: 1600552. 10.1002/mnfr.201600552

Tuncil YE, Thakkar RD, Arioglu-Tuncil S, Hamaker BR and Lindemann SR, 2018 Fecal microbiota responses to bran particles are specific to cereal type and in vitro digestion methods that mimic upper gastrointestinal tract passage. Journal of Agricultural and Food Chemistry 66: 12580–12593. 10.1021/acs.jafc.8b03469

Vandeputte D, Falony G, Vieira-Silva S, Wang J, Sailer M, Theis S, Verbeke K. and Raes J, 2017 Prebiotic inulin-type fructans induce specific changes in the human gut microbiota. Gut 66: 1968–1974. 10.1136/gutjnl-2016-313271 [PubMed: 28213610]

Vu VQ, 2011 ggbiplot: A ggplot2 based biplot. Available at: http://github.com/vqv/ggbiplot

Walters W, Hyde ER, Berg-Lyons D, Ackermann G, Humphrey G, Parada A, Gilbert JA, Jansson JK, Caporaso JG, Fuhrman JA, Apprill A. and Knight R, 2016 Improved bacterial 16S rRNA gene (V4 and V4–5) and fungal internal transcribed spacer marker gene primers for microbial community surveys. mSystems 1. 10.1128/mSystems.00009-15

Watson JA, Fang M. and Lowenstein JM, 1969 Tricarballylate and hydroxycitrate: substrate and inhibitor of ATP: citrate oxaloacetate lyase. Archives of Biochemistry and Biophysics 135: 209–217. 10.1016/0003-9861(69)90532-3 [PubMed: 5362924]

Wickham H, 2007 Reshaping data with the reshape package. Journal of Statistical Software 21: 1–20.

Wickham H, 2016 ggplot2: elegant graphics for data analysis. Springer-Verlag, New York, NY, USA 10.1007/978-0-387-98141-3

Wickham H, François R, Henry L. and Müller K, 2018 dplyr: A grammar of data manipulation. Available at: https://cran.r-project.org/web/packages/dplyr/index.html

Wilcoxon F, 1945 individual comparisons by ranking methods. Biometrics Bulletin 1: 80–83. 10.2307/3001968

Wolffram S, Badertscher M. and Scharrer E, 1994 Carrier-mediated transport is involved in mucosal succinate uptake by rat large intestine. Experimental Physiology 79: 215–226. [PubMed: 8003305]

Wu K, Li W, Song J. and Li T, 2015 Production, purification, and identification of Cholest-4-en-3-one produced by cholesterol oxidase from Rhodococcus sp. in aqueous/organic biphasic system. Biochemistry Insights 8: 1–8. 10.4137/BCI.S21580

Yang X, Twitchell E, Li G, Wen K, Weiss M, Kocher J, Lei S, Ramesh A, Ryan EP and Yuan L, 2015 High protective efficacy of rice bran against human rotavirus diarrhea via enhancing probiotic growth, gut barrier function, and innate immunity. Scientific Reports 5: 15004. 10.1038/srep15004

Yilmaz P, Parfrey LW, Yarza P, Gerken J, Pruesse E, Quast C, Schweer T, Peplies J, Ludwig W. and Glockner FO, 2014 The SILVA and ‘All-species Living Tree Project (LTP)’ taxonomic frameworks. Nucleic Acids Research 42: D643–648. 10.1093/nar/gkt1209 [PubMed: 24293649]

Zarei I, Brown DG, Nealon NJ and Ryan EP, 2017 Rice bran metabolome contains amino acids, vitamins & cofactors, and phytochemicals with medicinal and nutritional properties. Rice 10: 24 10.1186/s12284-017-0157-2 [PubMed: 28547736]

Zheng H, Yde CC, Clausen MR, Kristensen M, Lorenzen J, Astrup A. and Bertram HC, 2015 Metabolomics investigation to shed light on cheese as a possible piece in the French paradox puzzle. Journal of Agricultural and Food Chemistry 63: 2830–2839. 10.1021/jf505878a [PubMed: 25727903]

Zhou Y, Tozzi F, Chen J, Fan F, Xia L, Wang J, Gao G, Zhang A, Xia X, Brasher H, Widger W, Ellis LM and Weihua Z, 2012 Intracellular ATP levels are a pivotal determinant of chemoresistance in colon cancer cells. Cancer Research 72: 304 10.1158/0008-5472.CAN-11-1674 [PubMed: 22084398]

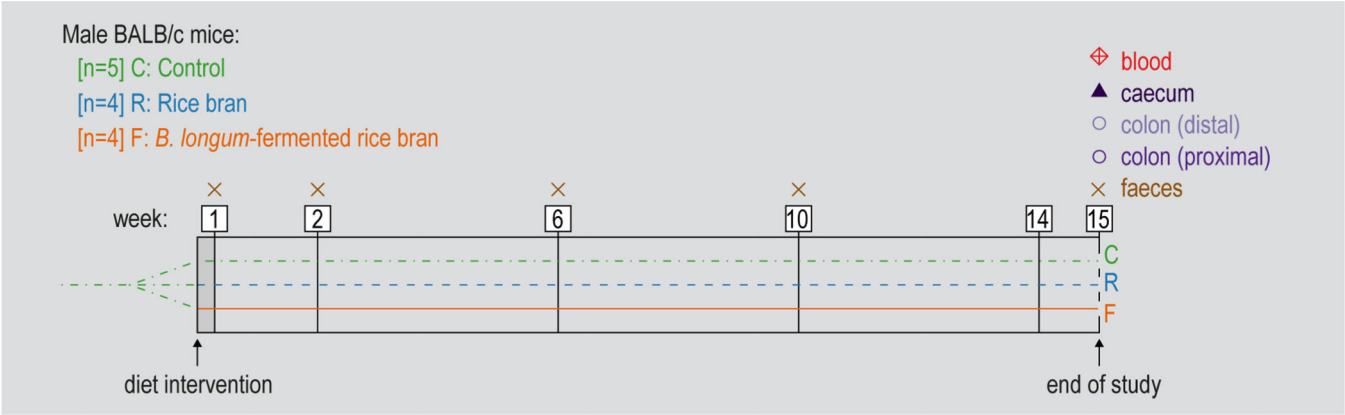

Figure 1.

Dietary intervention study design and timeline for tissue sampling in healthy mice. Male BALB/c mice were fed control, rice bran, or *Bifidobacterium longum*-fermented rice bran diets for 15 weeks. Faeces, caecum and colon were collected for microbiome analysis. Food, colon and blood samples were used for metabolite analysis.

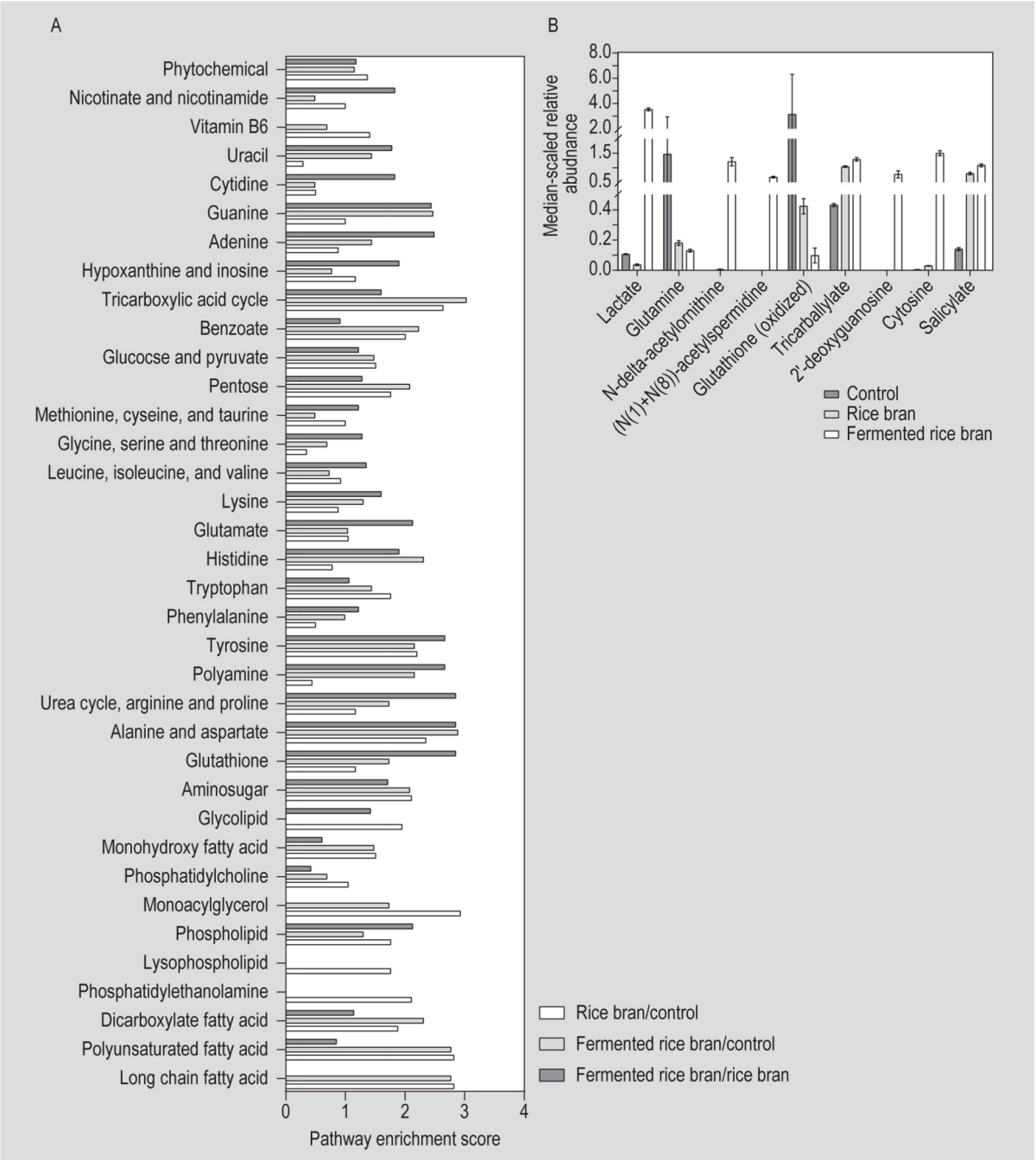

Figure 2.

The food metabolome differs across control, rice bran and *Bifidobacterium longum* fermented rice bran diets. (A) Pathway enrichment scores distinguishing control, rice bran and *B. longum* fermented rice bran diets. Metabolic pathways with a score of ≥1.0 for at least one or more treatment comparisons are listed. (B) Median-scaled relative abundances for selected metabolites that are significantly different between the three food metabolomes (P<0.05 when comparing abundance between two or more treatments).

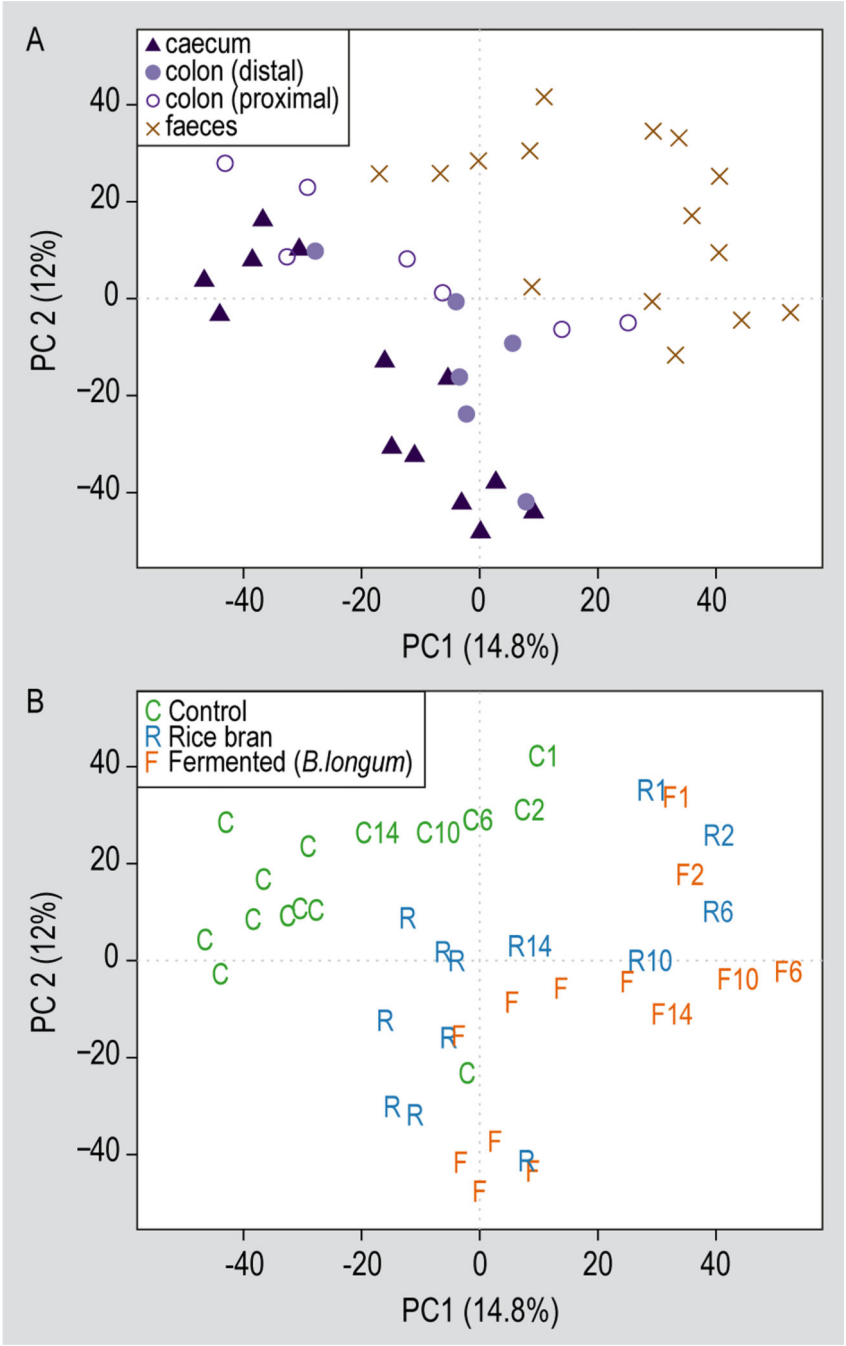

Figure 3.

Healthy murine microbiomes exhibit clear separation in community composition based upon sample type and diet group. Principal components analysis (PCA) of centred log-ratio transformed abundances for all amplicon sequence variants with abundance greater than two in faecal, colon, and caecum samples. Percentage values along each axis indicate the amount of variation explained by each of the first two principal components. (A) Symbols and colours denote sample type (faecal, caecum, distal or proximal colon). (B) Letters denote mouse diet group (control, rice bran, *Bifidobacterium longum*-fermented rice bran).

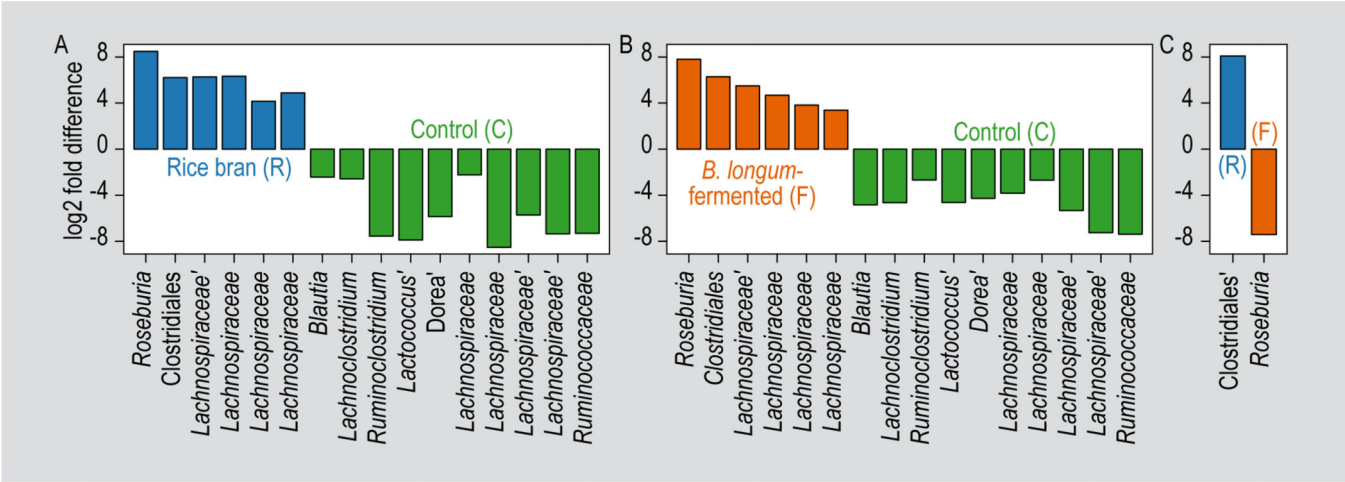

Figure 4.

Consumption of a rice bran or *Bifidobacterium longum*-fermented rice bran diet alters healthy murine microbiome composition compared to the control diet. Bar charts of log2 fold differences for sixteen differentially abundant (FDR-P<0.1) amplicon sequence variants; six ASVs exhibited conserved enrichment in mice fed rice bran or *B. longum*-fermented rice bran diets compared to control; 11 ASVs were conserved in control versus either experimental diet. Comparisons depicted in each panel are as follows: (A) rice bran vs control; (B) *B. longum*-fermented rice bran vs control; (C) rice bran vs *B. longum*-fermented rice bran. Bar colours denote mouse diet group. ASV taxonomic identities appended with the (‘) symbol indicate matched assignments for both Greengenes and SILVA databases; otherwise SILVA identity was specified.

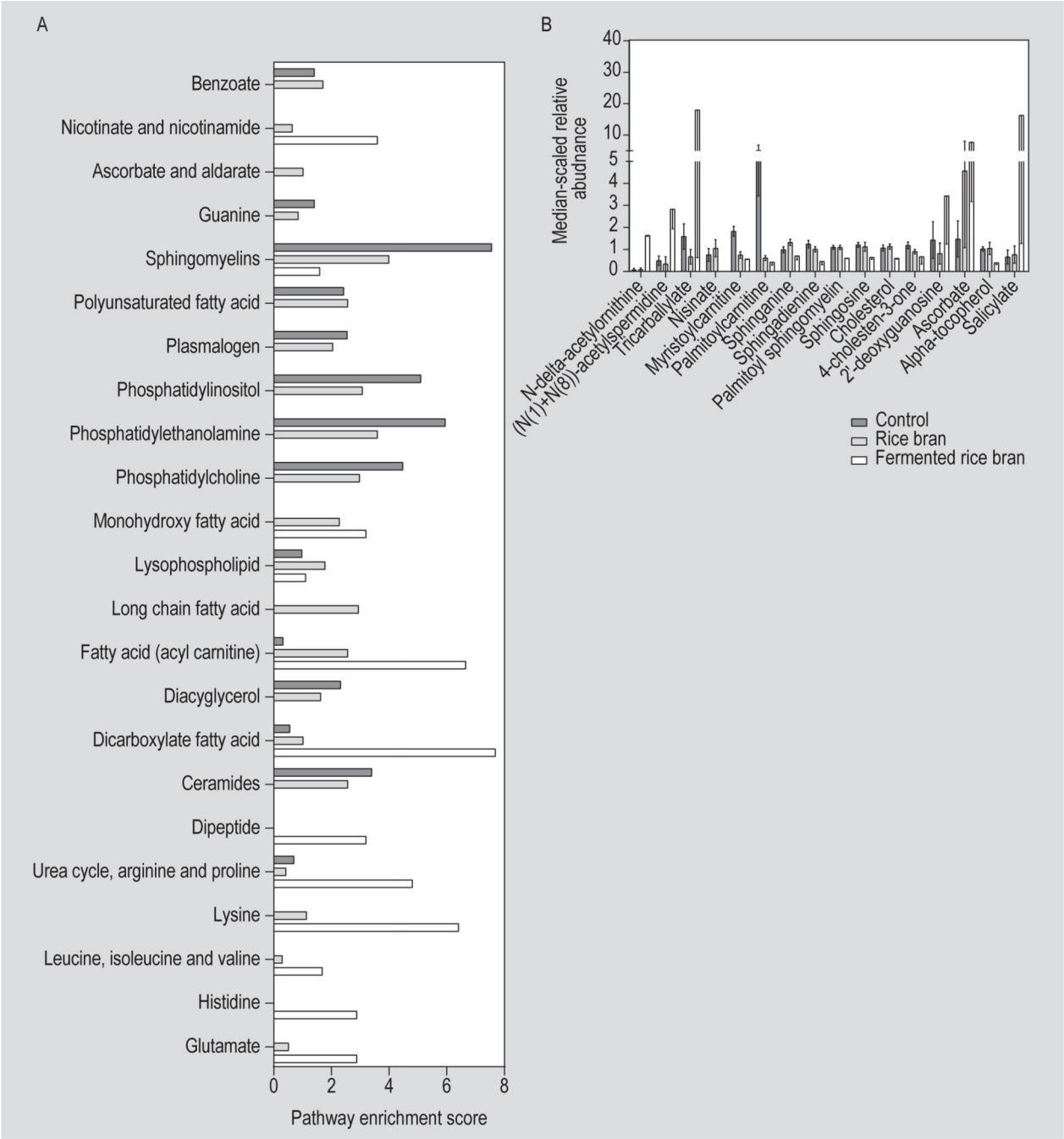

Figure 5.

Consumption of *Bifidobacterium longum*-fermented rice bran versus rice bran and control diets differentially modulate the colon tissue metabolome of healthy mice. (A) Pathway enrichment scores distinguishing the colon tissue of mice consuming the control, rice bran and *B. longum* fermented rice bran diets. Metabolic pathways with a score of ≥1.0 for one or more treatment are shown. (B) Median-scaled relative abundances for selected metabolites

distinguishing the three colon metabolomes. Depicted metabolites have a $P<0.05$ when comparing their abundance between two or more treatments.

Table 1.

Composition of mouse diets for each study group.

Constituents (g/kg)	**Control**	**10% rice bran**	**10% *B. longum*- fermented rice bran**
Casein	140.0	125.0	125.0
L-cystine	1.8	1.8	1.8
Corn starch	465.692	422.692	422.692
Maltodextrin	155.0	155.0	155.0
Sucrose	95.0	102.312	102.312
Corn oil	40.0	19.0	19.0
Cellulose	50.0	29.0	29.0
Mineral mix (with calcium and phosphate)	35.0	0	0
Mineral mix (without calcium and phosphate)	0	13.388	13.388
Calcium phosphate, dibasic	0	7.5	7.5
Calcium carbonate	0	6.8	6.8
Vitamin mix	15.0	15.0	15.0
Choline bitartrate	2.5	2.5	2.5
TBHQ, antioxidant[1]	0.008	0.008	0.008
Rice bran	0	100.0	0
B. longum-fermented rice bran	0	0	100.00

[1]TBHQ = tertiary butyl-hydroquinone.

Table 2.

Differentially abundant blood metabolites in mice consuming control, rice bran and *B. longum*-fermented rice bran diets.

Metabolic pathway[1]	Metabolites	Fold difference[2]		
		RB CON	FRB CON	FRB RB
Alanine and aspartate	N-acetylasparagine	↑1.35	↑1.81	↑1.33
Glutamate	glutamine	0.96	1.26	↑1.31
	pyroglutamine	1.33	↑2.07	1.56
Histidine	1-methyl-4-imidazole acetate	↓0.80	1.01	↑1.26
	3-methylhistidine	1.12	↑1.35	1.21
	anserine	↓0.63	0.76	1.21
Tryptophan	N-formylanthranilic acid	1.00	↑1.24	↑1.25
	picolinate	↑3.15	1.62	0.51
	indoleacetylglycine	↑2.56	↑2.52	0.98
Lysine	2-oxoadipate	↑1.56	1.07	↓0.69
Phenylalanine and tyrosine	tyrosine	0.84	1.10	↑1.32
	1-carboxyethyltyrosine	1.37	↑2.05	↑1.49
	N-acetyltyrosine	↓0.65	↓0.64	0.97
	phenol sulphate	↑3.44	↑6.02	1.75
	phenol glucuronide	2.91	↑5.02	1.72
	4-methoxyphenol sulphate	↑32.41	↑13.31	0.41
Methionine, cysteine, taurine	N-formylmethionine	1.03	↑1.27	↑1.24
	taurine	↓0.82	0.90	1.10
Urea cycle, arginine and proline	N-delta-acetylornithine	↑2.16	↑9.59	↑4.44
	N2,N5-diacetylornithine	-	↑2.09	↑2.09
Polyamine	5-methylthioadenosine	0.98	↑1.51	↑1.54
	(N(1) + N(8)-acetylspermidine	0.63	↓0.41	0.65
Glutathione	glutathione, oxidised	0.87	1.34	↑1.53
	ophthalmate	0.96	1.33	↑1.39
Dipeptide	valylglycine	↓0.29	0.84	↑2.87
Gamma-glutamyl amino acid	gamma-glutamylglycine	↑2.06	1.71	0.83
	gamma-glutamyl-epsilon-lysine	↑2.70	1.87	0.69

Metabolic pathway[1]	Metabolites	Fold difference[2]		
		RB CON	FRB CON	FRB RB
Pentose	arabitol/xylitol	0.91	↑1.34	↑1.48
	arabonate/xylonate	↓0.88	0.98	↑1.12
Aminosugar	N-acetylneuraminate	0.79	↓0.53	0.67
	N6-carboxymethllysine	↓0.60	0.72	1.19
Tricarboxylic acid cycle	alpha-ketoglutarate	2.74	↑3.49	1.27
Carnitine	propionylcamitine	1.26	↑1.93	↑1.53
	cis-4-decenoylcamitine	↓0.56	0.89	↑1.59
	methylmalonate	↑1.38	↑1.57	1.14
	acetylcarnitine	↓0.83	↓0.79	0.95
	3-hydroxyhexanoylcarnitine	↑1.10	1.07	0.97
	decanoylcarnitine	↓0.63	0.81	1.29
	myristoylcamitine	↓0.62	↓0.58	0.93
Long chain fatty acid	margarate	↑1.27	↑1.28	1.01
	stearate	↑1.07	↑1.07	1.01
	eicosanoate	↑1.62	1.40	0.86
Polyunsaturated fatty acid	arachidonate	1.18	↓1.51	↑1.28
	eicosapentaenoate	↑1.89	↑1.78	0.94
	docosahexaenoate	↑1.34	↑1.47	1.10
	docosatrienoate	↑1.64	1.27	0.77
	arachidonate	1.18	↑1.51	↑1.28
Branched fatty acid	15-methylpalmitate	↑1.29	↑1.25	0.97
Dicarboxylate fatty acid	Octadecenedioate[3]	↑2.82	↑3.82	↑1.36
	pimelate	↓0.31	↓0.28	0.91
	suberate	↓0.44	↓0.45	1.02
	azelate	↓0.19	↓0.14	0.77
	sebacate	0.79	↓0.61	0.76
	dodecadienoate	↓0.34	0.66	1.95
	octadecadeinedioate	↓0.46	0.71	1.55
Phopspholipid	choline	↓0.82	1.08	↑1.30

Metabolic pathway[1]	Metabolites	Fold difference[2]		
		RB CON	FRB CON	FRB RB
Plasmalogen	1-(1-enyl-palmitoyl)-2-linoleoyl-glycerophosphocholine	0.87	↓0.68	↓0.78
Monoacylglycerol	1-linoleoylglycerol	↑1.93	↑2.11	1.09
Diacylglycerol	oleoyl-oleoyl-glycerol [1][3]	0.76	↓0.27	↓0.36
	linoleoyl-linolenoyl-glycerol	↑3.72	2.29	0.62
	stearoyl-arachidonoyl-glycerol	↓0.49	↓0.35	0.70
	hexadecasphingosine	↓0.54	↓0.58	1.07
	heptadecasphingosine	↓0.68	↓0.68	0.99
Ceramide	ceramide (d18:1/17:0, d17:1/18:0)[3]	0.45	↓0.33	0.74
Endocannabinoid	oleoyl ethanolamide	1.21	↑1.51	1.25
Sterol	7-alpha-hydroxy-3-oxo-4-cholestenoate	1.01	↑1.16	↑1.15
	campesterol	↓0.75	↓0.73	0.97
Primary bile acid	chenodeoxycholate	0.66	1.18	↑1.79
Secondary bile acid	deoxycholate	↓0.78	1.17	↑1.49
Uracil	N-acetyl-beta-alanine	↓0.69	↓0.14	↓0.20
	uridine-5'-monophosphate	0.67	↓0.46	0.69
Xanthine and inosine	Inosine 5'-monophosphate	↓0.54	0.72	1.35
Cytidine	cytosine	1.14	↑6.48	↑5.67
	5-methylcytidine	↓0.52	↓0.45	0.88
Nicotinate and nicotinamide	trigonelline	↓51.32	↑70.30	1.37
	N1-methyl-2-pyridone-5-carboxamide	↓0.40	0.65	1.60
Phytochemical	2-hydroxyhippurate (salicylurate)	↑9.89	↑22.46	↑2.27
	thioproline	1.33	1.02	↓0.77
	hippurate	↑3.79	↑4.17	1.10
	4-hydroxyhippurate	↑4.07	↑3.24	0.80
	catechol sulphate	↑3.11	↑3.52	1.13
	4-methylcathecol sulphate	↑4.66	3.74	0.80
	4-vinylphenol sulphate	↑6.57	↑5.25	0.80
	3-phenylproprionate	1.85	↑4.19	2.27
	2,3-dihydroxyisovalerate	1.29	↑1.46	1.14

Metabolic pathway[1]	Metabolites	Fold difference[2]		
		RB CON	FRB CON	FRB RB
	caffeic acid sulphate	↑3.61	↑5.13	1.42
	2-oxindole-3-acetate	1.42	↑3.99	2.81
	ferulic acid 4-sulphate	↑80.32	↑73.77	0.92
	N-glycolylneuraminate	0.79	↓0.57	0.73
	stachydrine	↑4.44	↑2.55	0.57
	tartarate	↑3.87	3.06	0.79
	N-acetylpyrraline	↑1.85	↑2.60	1.41
Other	ergothionine	0.93	↑1.65	↑1.77
	erythritol	↑1.35	↑1.77	↑1.32
	salicylate	↑5.88	↑6.57	1.12
	ethyl-glucuronide	2.21	↑8.68	3.92
	1,2,3-benzenetriol sulphate	↑5.66	2.31	0.41

[1] Table displays metabolites from metabolic pathways with an enrichment score of ≥1.0 for at least one treatment comparison.

[2] FRB = fermented rice bran; RB = rice bran.

[3] Indicates metabolite annotation was not made via an internal Metabolon library standard but predicted using spectral profiles from curated chemical databases.